Mathematical and Computational Applications

MDPI

Article

Evaluation of the Impact of Stress Distribution on Polyurethane Trileaflet Heart Valve Leaflets in the Open Configuration by Employing Numerical Simulation

Lebohang Reginald Masheane [1,*], Willie du Preez [2] and Jacques Combrinck [1]

[1] Department of Mechanical and Mechatronics Engineering, Faculty of Engineering, Build Environment and Information Technology, Central University of Technology Free State, Bloemfontein 9300, South Africa; jcombrinck@cut.ac.za

[2] Centre for Rapid Prototyping and Manufacturing, Faculty of Engineering, Build Environment and Information Technology, Central University of Technology Free State, Bloemfontein 9300, South Africa; wdupreez@cut.ac.za

* Correspondence: lmasheane@cut.ac.za; Tel.: +27-51-507-3683

Abstract: It is costly and time-consuming to design and manufacture functional polyurethane heart valve prototypes, to evaluate and comprehend their hemodynamic behaviour. To enhance the rapid and effective design of replacement heart valves, to meet the minimum criteria of FDA and ISO regulations and specifications, and to reduce the length of required clinical testing, computational fluid dynamics (CFD) and finite element analysis (FEA) were used. The results revealed that when the flexibility of the stent was taken into consideration with a uniform leaflet thickness, stress concentration regions that were present close to the commissural attachment were greatly diminished. Furthermore, it was found that the stress on the leaflets was directly impacted by the effect of reducing the post height on both rigid and flexible stents. When varying the leaflet thickness was considered, the high-stress distribution close to the commissures appeared to reduce at thicker leaflet regions. However, thicker leaflets may result in a stiffer valve with a corresponding increase in pressure drop. It was concluded that a leaflet with predefined varying thickness may be a better option.

Keywords: polyurethane heart valve; finite element analysis; stress concentration regions; geometric orifice area

check for updates

Citation: Masheane, L.R.; du Preez, W.; Combrinck, J. Evaluation of the Impact of Stress Distribution on Polyurethane Trileaflet Heart Valve Leaflets in the Open Configuration by Employing Numerical Simulation. *Math. Comput. Appl.* **2024**, *29*, 64. https://doi.org/10.3390/mca29040064

Academic Editor: Sebastian Skatulla

Received: 31 May 2024
Revised: 23 July 2024
Accepted: 6 August 2024
Published: 10 August 2024

Copyright: © 2024 by the authors. Licensee MDPI, Basel, Switzerland. This article is an open access article distributed under the terms and conditions of the Creative Commons Attribution (CC BY) license (https://creativecommons.org/licenses/by/4.0/).

1. Introduction

A typical tricuspid aortic valve consists of three semilunar leaflets, and it is situated between the ascending aorta and the left ventricular outflow tract. The cusps (leaflets) open during systole to let blood flow from the ventricle into the aorta, and they close during diastole to stop blood from flowing backwards [1]. Two separate valve diseases that can be distinguished are aortic stenosis and aortic insufficiency during the operation of the valve. The disorder known as calcified aortic valve stenosis is characterized by the buildup of calcium in tissues and the thickening of mineral conglomerates, which impede blood flow [2]. When aortic stenosis occurs, the blood flow from the left ventricle to the aorta is impeded due to narrowing of the left ventricular outflow tract around the aortic valve, resulting in the pressure gradient between the two rising sharply. Insufficiency due to regurgitation of blood from the aorta into the cavity of the left ventricle occurs when the aortic valve leaflets do not close completely during diastole [2,3]. Severe insufficiency is thought to cause the left ventricle to resorb up to 60% of the systolic blood volume. Continuous severe regurgitation will eventually cause an abrupt rise in left ventricle diastolic pressure and a reduction in cardiac output [3–5].

Heart valve replacement is often less favourable than repair but is necessary in severe cases. However, this procedure is costly, and due to the limited lifespan of the commercially available prosthetic valves, it tends to be uncomfortable, particularly for patients who

undergo multiple surgeries [6,7]. In Sub-Saharan Africa and the developing world, there is an unmet need of 33 million people under the age of 65 who suffer from rheumatic heart valve disease, to produce an inexpensive prosthetic valve that requires little to no use of anticoagulant therapy and has an equivalent, if not superior, lifespan to that of a commercially available biological valve [8]. Over recent decades, much research has been performed on the potential replacement of mechanical and biological heart valves with polymeric heart valves. The latter have favourable flow dynamics and physical characteristics when compared to human heart valves; however, it is frequently unpredictable how well a polymer heart valve will perform in terms of flexibility, longevity, and hemodynamic performance [9–11].

According to ISO 5840-3 [12], which establishes hydrodynamic function requirements for heart valves, an effective orifice area (EOA) must exceed 0.85 cm^2, along with a transvalvular regurgitant fraction of less than or equal to 10%, and an overall regurgitant fraction of less than or equal to 20%, are mandatory. Valves must operate under pulsatile flow for at least 200 million cycles, or five years, at a consistent pressure differential of 100 mmHg across the closed aortic valve. Furthermore, the condition must be satisfied in more than 95% of test cycles [12].

For many researchers, using a pulse duplicator system for in vitro testing of heart valves has become standard procedure. Under standardized hemodynamic settings, the device is capable of measuring regurgitant fraction, mean pressure gradient, and EOA [7,13–15]. In comparison to the commercially available Carpentier-Edwards Perimount Magna 19 mm valve, the present trileaflet polycarbonate urethane (PCU) valve design of the authors demonstrated the capacity to provide an equivalent overall hemodynamic performance. The findings of this early in vitro study suggest that the leaflet and stent material, stent design and flexibility, and manufacturing processes may have an impact on how well the PCU trileaflet valve functions [16]. Here, we conducted an investigation to determine the optimal combination of these variables to be incorporated into leaflet design that will have the greatest influence on valve durability and performance. Replication of the experimental pulse duplicator system in the digital environment by utilizing CFD modelling for testing a valve to ascertain the influence of the individual abovementioned parameters on PCU valve von Mises stresses, geometric orifice area (GOA), and coaptation region will yield considerable design time and cost savings.

An aortic valve substitute must exhibit robust mechanical characteristics to sustain its basic functions under the complicated cyclic shear–flexural–tensile stress present in the blood environment. Intercommissural leaflet distances increase with ventricular pressure, creating a tangential strain that pulls the leaflets apart. The impact of high-speed fluid on the leaflets produces shear stress, whereas large tensile stress is created by pressure differences across valves. Furthermore, flexural stresses are brought on by the fluctuating fluid flow that opens and closes the leaflets, even if it is only for short periods. Within the last few decades, medical device researchers have displayed a growing enthusiasm for CFD and FE techniques to examine how frame mobility affects the shape and stress–strain condition of the curvature of a valve leaflet [15,17–19]. However, technical challenges regarding the precision of such simulations are related to using constitutive models that correctly represent the mechanical characteristics of materials. Additionally, reference input for a parameter estimation algorithm frequently originates from experimental data.

The mechanical properties of pericardial valves have been extensively evaluated and characterised in recent decades by multiple groups in an effort to increase their longevity. However, prediction of the behaviour of these materials has been classified as linear isotropic, nonlinear isotropic, linear anisotropic, and nonlinear anisotropic [1,13,15,17,20–23]. Certainly, these valves will provide a distinct stress and strain distribution in leaflets when simulated. In their FE analysis, Rousseau et al. [24] used fibre reinforcement and viscoelasticity as properties of a porcine bioprosthetic valve leaflet. They then applied a time-varying pressure load on the leaflets and discovered a correlation between certain common regions of valve failure and regions of high fibre stress, which were located close to the aortic ring.

It is essential to comprehend the mechanical characteristics of PCU material, such as its elastic modulus, yield strength, and fatigue behaviour, in order to forecast the distribution of stress inside the valve and evaluate its long-term effectiveness.

The current study aimed to utilize computational simulation to give predicted data that modern imaging methods are unable to supply, and to examine the intricate biomechanics of the prosthetic aortic valve. A previously designed and manufactured valve, hemodynamically tested, was selected, and simulations were used in an effort intended to contribute to and advance valve design by systematizing knowledge about the impact of every parameter on the hemodynamic efficiency of a heart valve by comparing the GOA, coaptation area, and stress distribution.

2. Materials and Methods

2.1. Valve Design

A comprehensive analysis was conducted of the characteristics and functioning mechanism of the reverse-engineered PCU valve, as well as the failure mechanisms seen in in vitro research using tissue valves. Figure 1a shows the leaflet dip-moulding tool that was defined in a closed position by analysing a commercially available biological valve (Carpentier-Edwards Perimount Magna 19 mm) utilizing reverse engineering techniques. The valve design consists of 3 symmetrical thin leaflets that are affixed to a cylindrical supporting frame, often known as a stent. The stent is equipped with three posts that provide support for the flexible leaflets [25].

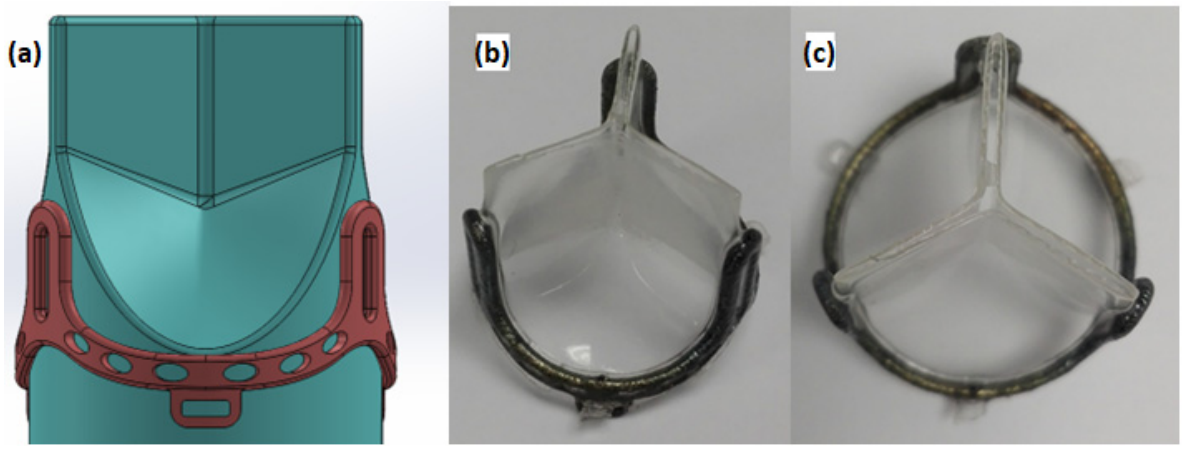


Figure 1. Trileaflet PCU valve produced with dip-moulding process without final trimming. (**a**) Dip-moulding tool; (**b**) side view of the valve prototype; (**c**) top view of the valve prototype.

The SolidWorks software 2024 (Dassault Systèmes SolidWorks Corp., Waltham, MA, USA) was used to create a computer-aided design (CAD) model of the trileaflet valve, which consisted of a stent with three posts, where PCU leaflets were attached. Initially, the leaflets thickness was modelled as a uniform 100 µm thickness, whereas the stent's thickness was assigned as 0.1 cm. The material properties of PCU exhibit a stress–strain relationship that is nonlinear and may be well characterised using an isotropic hyperelastic model. The neo-Hookean isotropic model was selected for the material response and assumed to be nearly incompressible. The mechanical characteristics of the PCU were enhanced by including nonlinear geometry and implicitly unsteady behaviour. A saline–glycerol composition consisting of 47.3% saline and 52.7% distilled water was chosen to attain a density of 1132 kg/m^3 which is similar to that of blood and was assumed to be Newtonian. The blood is classified as non-Newtonian fluid; however, it ceases to exhibit this characteristic at a shear rate beyond 100–200 s^{-1} [26]. Polymer leaflets were manufactured to produce a bulk modulus of 53.33 MPa, while Poisson's ratio was set to 0.45, with a density of 830 kg/m^3. The stent was designed with Young's modulus of 113.8 GPa and a density of 4430 kg/m^3.

2.2. FE Simulation

As part of the design verification process, a computational model to study the structural deformation of the valve leaflets was developed utilizing STAR CCM+ 2322 software, and simulation outcomes were compared with the hemodynamic performance of a dip-moulded PCU valve [16,25]. The dynamic behaviour of the PCU trileaflet valve, including the dynamic deformation, leaflet coaptation area, and stress distribution, were investigated for two distinct cases, which are a model with a rigid stent and one with a flexible stent. The radial displacement of the inner leaflet surface was constrained. In the contact model, the frictionless coefficient was set. A preliminary simulation was conducted with the attachment curvature of the leaflet onto the stent constrained, to assess the effect of the rigid stent on the leaflet's dynamics.

Directed mesh operation that defines a quadrilateral mesh on the surface of the leaflet was selected. Time-varying aorta–ventricular pressure gradient loading over a full cardiac cycle of 0.83 s on the valve leaflets was obtained during the investigations of the hemodynamic performance of the valve through the in vitro experiments [16,25].

3. Results

3.1. Assessment of Leaflet Deformation

To investigate the effect of rigid and flexible stents, three specific characteristics were chosen for analysis: GOA, coaptation area, and stress distribution. To quantify valve stenosis throughout the cardiac cycle, the GOA was used as the measure of the effective flow area instead of EOA. The applied pressure load to the leaflet is transferred to the commissures since the central section of each leaflet is attached to it. Hence, quantifying the coaptation area would provide valuable insights about the efficiency of the coaptation profile. Calcific degeneration often occurs in locations where leaflet stresses are higher. Therefore, such knowledge would be beneficial in determining the longevity of the valve.

3.1.1. Geometric Orifice Area

The maximum value of the GOA assists in predicting and improving the hemodynamic performance of the valve. The GOA was calculated by measuring the orifice areas of each valve that were captured in the FEA simulation in its completely open deformation state during the loading cycle. Figure 2 shows how the GOA of uniform 100 µm thickness varies for both rigid and flexible stents.

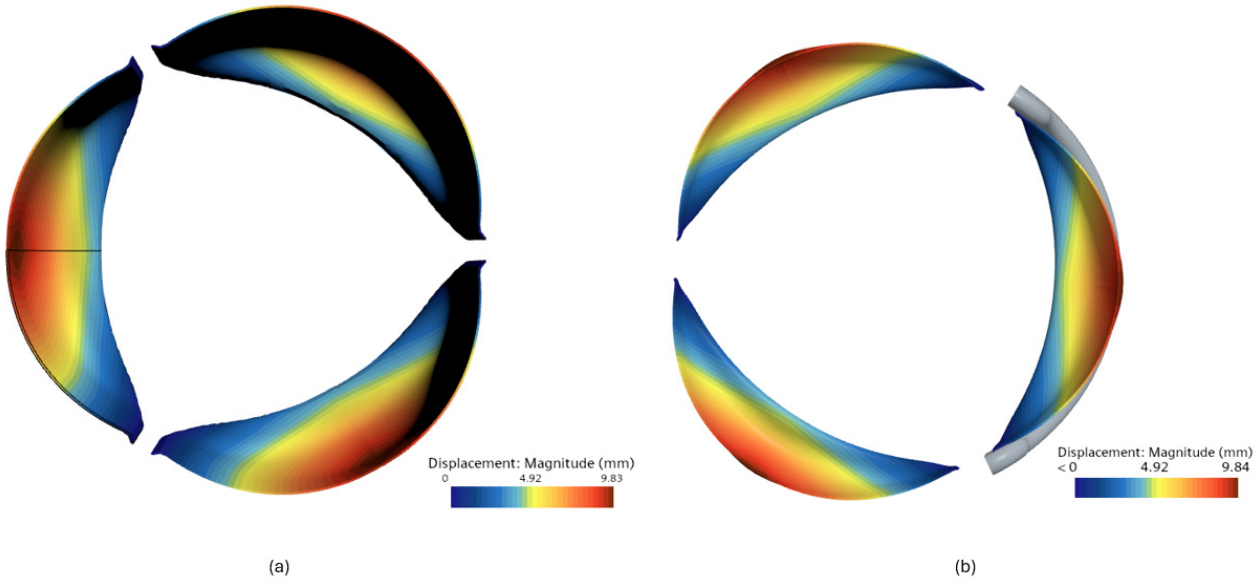


Figure 2. GOA captured in the FEA simulation of a uniform 100 µm leaflet thickness for (**a**) rigid and (**b**) flexible stents.

The maximum GOA for a rigid stent was determined to be 303 mm^2, while the flexible stent valve showed a notable 25% increase in GOA with a value of 378.8 mm^2. However, when in the diastole phase, both valves showed a similar leaflet gap.

3.1.2. Coaptation Zone

Figure 3 depicts the deformation that occurred in the PCU leaflet models. When examining the deformation of a leaflet attached to a rigid and flexible stent that was assigned 0.1 cm thickness, respectively, with uniform leaflet thickness, it was observed that at the particular coaptation height (a region of a leaflet that hangs below the free edges of the opening leaflet), folding of the material was present. This conduct of the material will create an obstruction that will hinder the blood circulation, resulting in a pressure drop and an increase in regurgitation fraction.

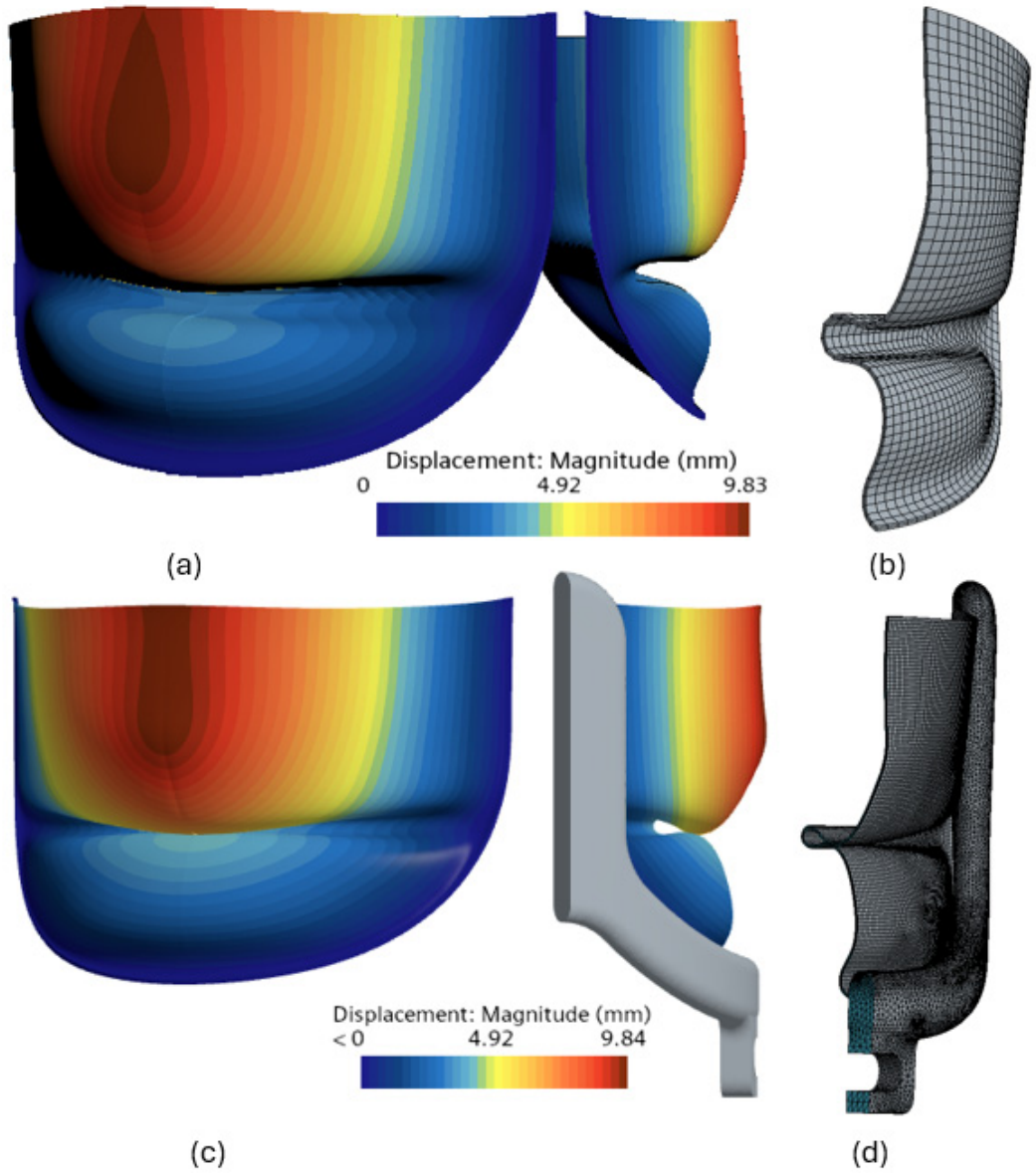


Figure 3. Structural FEA comparing leaflet deformation at the coaptation area of a uniform 100 µm leaflet thickness. (**a**) Side view of a simulation in which the stent is rigid; (**b**) cross-section of a simulation in which the stent is rigid; (**c**) side view where the stent is flexible; (**d**) cross-section where the stent is flexible.

Additionally, with the same design but with adjustment to the stent boundary condition, it can be observed in Figure 3c,d that a contact around the deformed leaflet was detected on the flexible stent.

3.1.3. Stress Distribution

Figure 4 shows the von Mises stress distribution within the leaflets for the two types of stents with a uniform 100 µm leaflet thickness. The models for both the rigid and the flexible stent exhibited peak stress distribution near the commissures and on the curvature of the attachment. In Figure 4a, it is clear that the high-stress concentrations displayed in the vicinity of the valve belly correspond to the regions where the minimum thickness of the leaflet was measured.

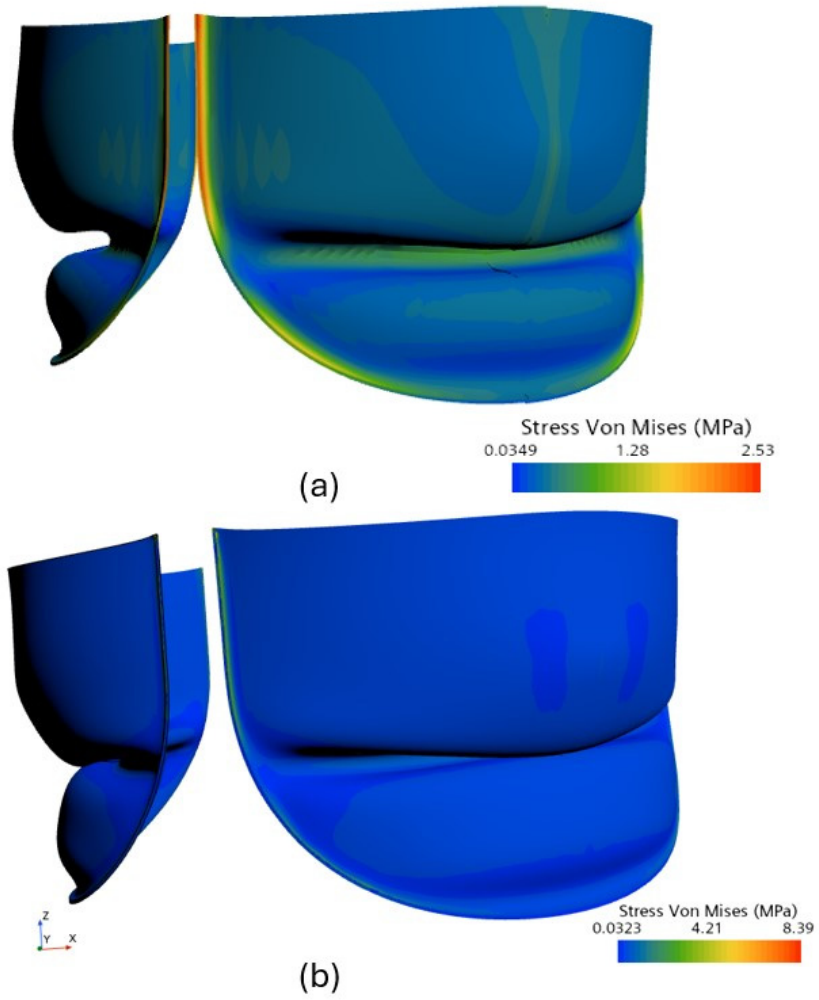


Figure 4. The von Mises stress distribution (MPa) of a uniform 100 µm leaflet thickness was calculated for two distinct boundary condition models at the instant of complete valve opening. (**a**) Rigid stent valve; (**b**) flexible stent valve.

However, unlike the case of a rigid stent, the valve with a flexible stent (Figure 4b) showed a distribution of reduced stress at all areas of the configuration.

3.2. Stent Post Height

To assess the effect of stent post height, three alterations were implemented to the stent design, and each stent design was allocated a name to mitigate any potential confusion arising from diverse simulations (see Figure 5).

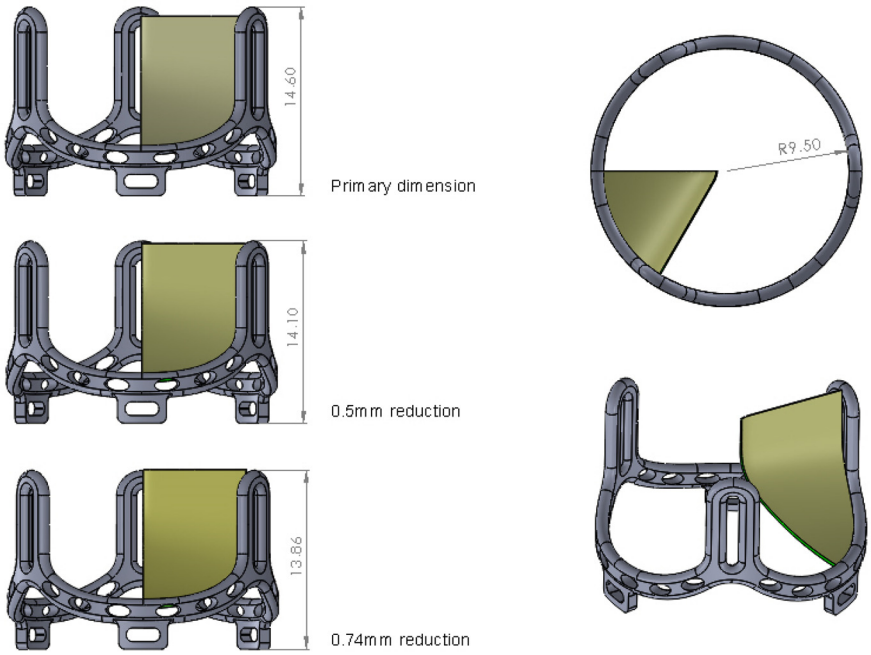


Figure 5. Optimizing the stent design to assess the effectiveness of post height. Dimensions in mm.

Table 1 shows the results of the GOA and the maximum stress at different stent post heights. In all three studies, the leaflet geometry of a uniform 100 µm leaflet thickness and material properties were kept the same.

Table 1. The GOA and stress distribution results of different stent post heights.

Stent Post Height	GOA (mm^2)	Maximum Stress (MPa)
Primary dimension	303	8.39
0.5 mm reduction	307	8.82
0.74 mm reduction	308	9.03

The valve equipped with a 0.74 mm reduction in the stent post height demonstrated the largest GOA, measuring 308 mm^2, while the valve with the primary dimension surpassed all other valves by showing the lowest maximum stress of 8.39 MPa. The study revealed a correlation between decreasing the post height and an increase in both the GOA, as well as the maximum stress at the unrestricted border of the valve.

3.3. Effect of a Dip-Moulded Varying Leaflet Thickness

In the process of manufacturing valve leaflets, dip moulding produces a varying leaflet thickness, while compression moulding offers the opportunity to manufacture valves with predefined uniform or varying thicknesses. To predict which of the manufacturing techniques should be employed, an investigation to compare the effects of these two types of leaflet thickness was launched.

3.3.1. Comparison of Coaptation Area

In Figure 6, the results of structural deformation at the coaptation area are shown. The valve simulations in Figure 6 have discernible leaflet curvature at a certain coaptation height when completely open. The thinner thickness at the belly of the uniform thickness valve (Figure 6a) exhibited a wrinkled leaflet which would encounter increased bending stress that might reduce the lifespan of the valve. This folding site would also contribute to higher pressure loading demand during the diastole phase.

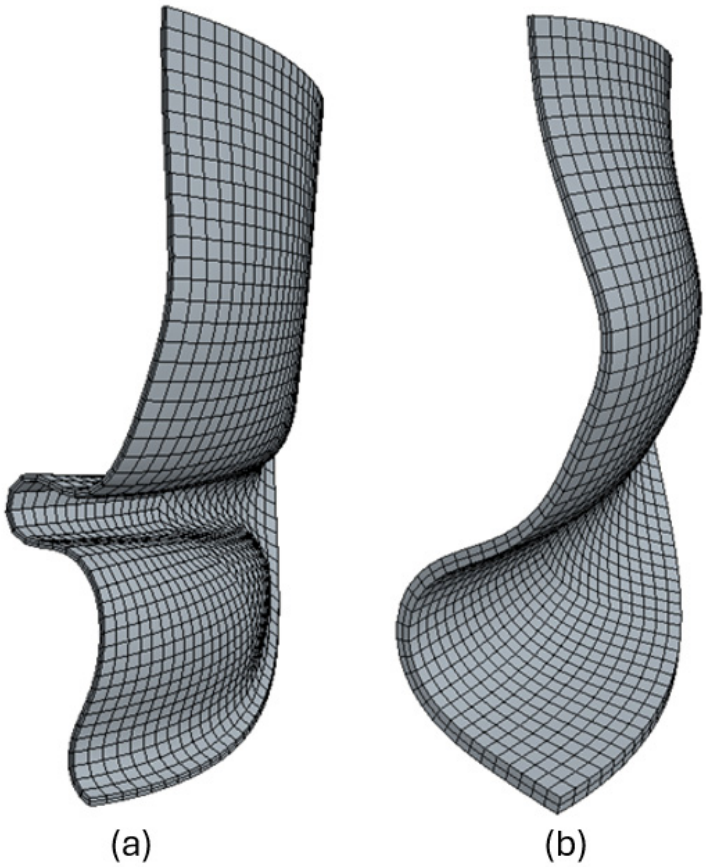


Figure 6. Structural FEA comparing leaflet deformation at the coaptation area of (**a**) simulation in which the leaflet thickness was a uniform 100 μm and (**b**) where the leaflet was varied from 70 to 280 μm, obtained through the dip-moulding production process.

The dip-moulding process produces a component that has interior dimensions and shapes identical to the external dimensions of the mould. During the curing process, the polymer liquid flowed over the mould surface due to the force of gravity, resulting in accumulation of a 280 μm thick film in the lowest regions. This led to the formation of a valve that had a greater thickness towards the base, which progressively decreased in thickness immediately after the valve belly to 70 μm. Thereafter, the thickness reached 110 μm at its highest point near the coaptation area. Increasing the thickness at the valve's belly and below, as shown in Figure 6b, indicates a potentially stiffer belly region, which would prevent the leaflet from wrinkling while opening, but the thinner thickness above the valve belly increased the coaptation area. This evaluation provides a more accurate insight into the initial behaviour of the dip-moulded valve in comparison to modern imaging techniques such as fluoroscopy, particle image velocimetry, and cardiovascular magnetic resonance. With these techniques it is difficult to provide 3D spatial information, and the ability to identify small, highly mobile objects is lacking due to image acquisition over multiple cardiac cycles [27,28]. The current evaluation also deepens the comprehension of how a predefined leaflet thickness might enhance the functionality of the valve.

3.3.2. Stress Distribution for Varying and Uniform Leaflet Thickness

Figure 7 shows the results of evaluating the von Mises stress distribution for uniform and varying leaflet thicknesses. In comparison with uniform leaflet thickness, a varying leaflet thickness shown in Figure 7d demonstrates a decrease in stress concentration at the attachment point of the leaflet onto the stent towards the base of the valve. However, a notable rise in stress concentration is found just above the valve's belly.

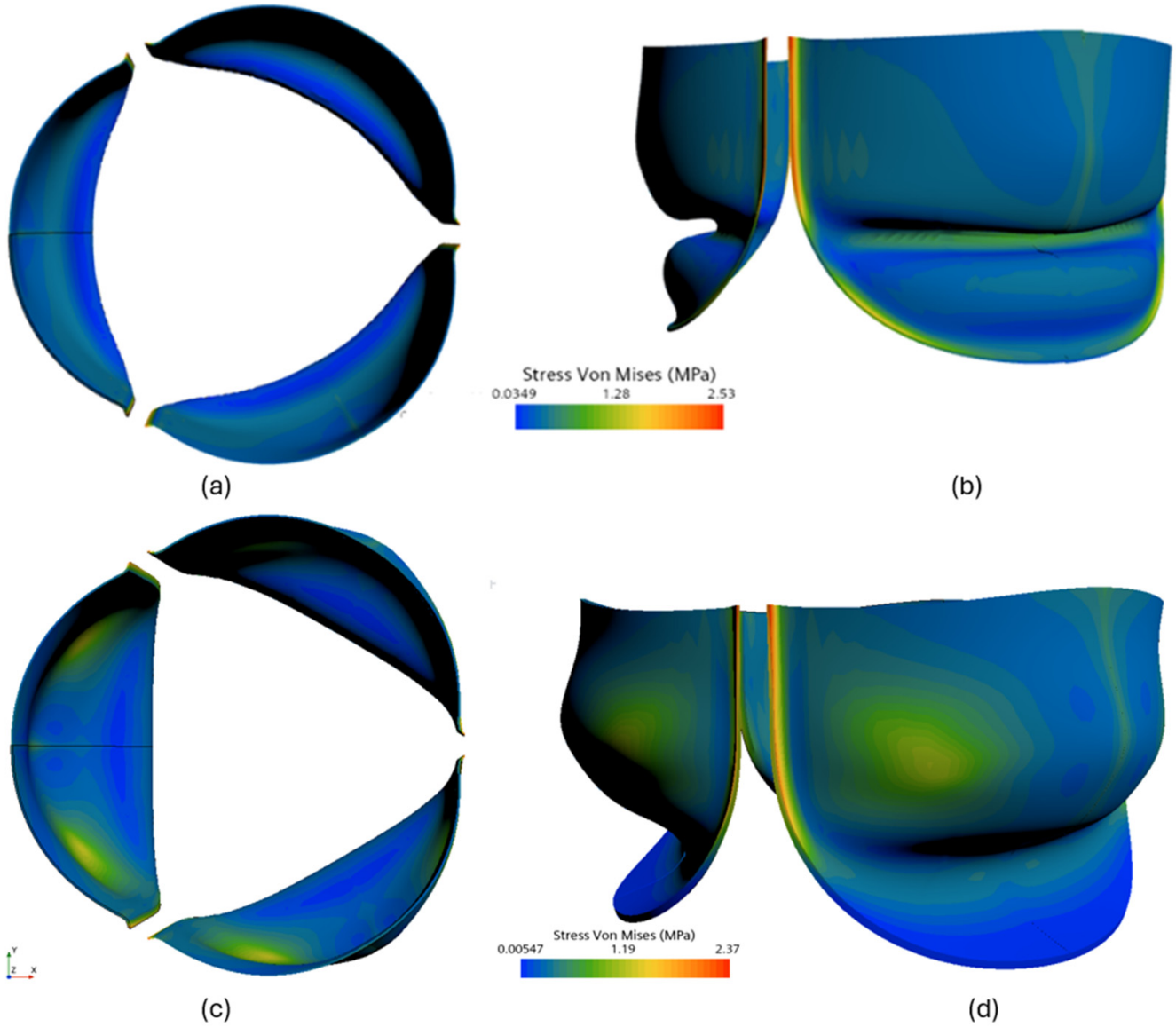


Figure 7. The von Mises stress distribution (MPa) was calculated for two distinct leaflet thickness models at the instant of complete valve opening. (**a**) Top view of a 100 µm uniform thickness; (**b**) side view of a 100 µm uniform thickness; (**c**) top view of varying thickness ranging from 70 to 280 µm; (**d**) side view of varying thickness ranging from 70 to 280 µm of the valve leaflets.

These simulations demonstrate that leaflet thickness has an impact on the pressure loading experienced during the cardiac cycle. As a result, the fatigue characteristics of the distinct regions of the leaflet would probably vary significantly.

3.3.3. Effect on GOA

The correlation between leaflet thickness and the displacement of the valve is illustrated in Figure 8. With the same design and boundary conditions, there is a notable improvement in GOA for varying leaflet thickness (see Figure 8b). In addition, the results show that a 30 µm decrease in the thickness just above the belly leads to a 2.7% rise in the displacement above the belly of the valve, in comparison to the 9.83 mm displacement achieved by the uniform thickness.

It is expected that this functional advantage would minimize the leaflet opening pressure, regurgitation fraction, and energy loss.

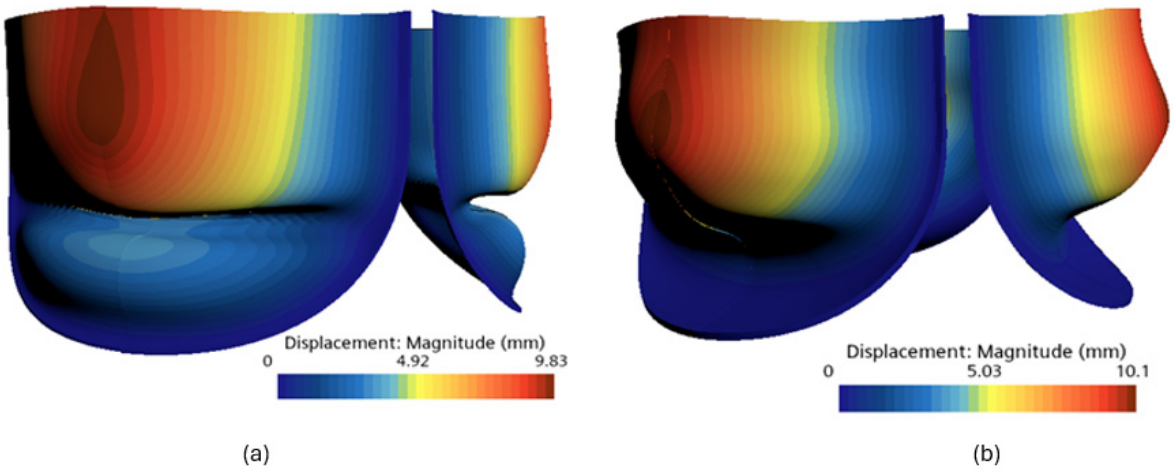


Figure 8. The side view of PCU valves when completely open. (**a**) A 100 μm uniform leaflet thickness; (**b**) varying leaflet thickness ranging from 70 to 280 μm.

4. Discussion

The process of pathological calcification, which influences valve durability, has been demonstrated by earlier researchers to be influenced by mechanical stress [29–31]. Furthermore, structural deformation has been hypothesised to potentially contribute to the valve calcification. Additionally, significant deformation of the prosthetic heart valve stent affects stress distribution. Consequently, the valves become more vulnerable to leaflet thrombosis and could experience premature structural degradation [29–31]. This study evaluated the stress distribution in the valve leaflets by computing half of the cardiac cycle. Data on the von Mises stress were acquired for the mechanical performance quantification of the valves to facilitate design optimization. The maximum stress during the complete systole phase was found in close proximity to the commissures and the curvature of the leaflet attachment onto the stent. A study conducted by Tao, L. et al. [32] identified the maximum von Mises stress after calculating a complete cycle to be 0.695 MPa located at the commissure tips. To reduce this stress, the process of dividing and thickening the areas on the valve with high stress concentration was repeated by them for four iterations. On iteration 4, the maximum thickness was lowered to 0.499 MPa at a maximum thickness reaching 0.65 mm, resulting from 0.1 mm thickness on each increment [32]. However, the increase in the leaflet thickness also has a direct impact on the flexibility of the leaflets, which subsequently hinders their displacement. An optimal balance between valve flexibility to perform natural functions while remaining durable must be thoroughly examined. The present assessment revealed that the use of a flexible stent can effectively reduce the stress concentration from 2.53 MPa, which occurred in the curvature of the leaflets connected to the stent, to 1.03 MPa.

Polymer heart valves are designed and developed to address the limitations of mechanical and bioprosthetic valves, such as thrombogenic complications and fatigue-related issues. Optimizing the stress distribution in polymer heart valves remains a crucial parameter to improve valve longevity. Through the numerical analysis of the impact of varying leaflet thickness, it was identified that the thinner region near the valve's belly would encounter a significant stress concentration, making it prone to fatigue and failure of the valve. The thicker regions of the valve leaflets demonstrated a significant reduction in stress concentration, therefore enhancing the fatigue resistance of the polymer heart valves. This emphasised the need for further study, whereby a progressive thickening of the leaflets at the most affected areas to minimize stress concentration, while maintaining the functional requirements of this valve, must be conducted.

The research conducted by Yousefi et al. [33] revealed that a higher stent profile reduced regurgitation flow. In the current study, it was found that increasing the post height significantly reduced the maximum stress on the free edges of the leaflets; however, this decreased the GOA of the valve. The GOA determines the anatomical opening size

for the blood flow through the valve. The smallest post height of the stent resulted in a measured GOA of 3.03 cm^2. The blood flow downstream of the valve produces a vena contracta, the location where the EOA is measured. As previously stated, according to ISO 5840-3, a valve with 19 mm diameter is required to have an EOA exceeding 0.85 cm^2. Based on the previous in vitro experiments, this 3.03 cm^2 GOA led to a valve meeting the minimum EOA specified by the ISO standard. However, a stent redesign that enables a watertight valve closing, exhibits an expanded coaptation region, and minimizes the stress concentrations would be beneficial.

In a previous study, it was shown that inadequate coaptation was also a fundamental mechanistic factor contributing to valve regurgitation [16]. Ensuring optimized leaflet deformation is another crucial parameter in reducing the amount of regurgitation. Uniform thickness displayed a poor performance due to the losses from the turbulence in the central flow emanating from the wrinkled leaflet. This turbulence would lead to increased haemolysis and platelet activation. Despite the attempts to create a uniform leaflet thickness, this study suggests that a leaflet with predefined varying thickness may be a better option.

The dip-moulding procedure resulted in prototypes with an overall undetermined leaflet thickness. The region near the valve's belly had a thinner thickness, resulting in a higher stress concentration in that area. An optimally controlled variable thickness, which minimises stress concentration and allows flexibility, is expected to improve the hemodynamic performance and lifetime of the valve. To meet the design-for-manufacturing requirements, it is proposed to use compression moulding as the production technique. This process is economically efficient and can produce predefined leaflet thicknesses.

5. Conclusions

Application of CFD and FEA simulations has emerged as a useful tool in the design process of a polyurethane heart valve. The stress concentration, GOA, and coaptation region were evaluated in relation to structural analysis when the leaflet thickness, flexibility, and profile height of the stent changed. A rigid stent simplified the analysis and reduced computational cost; however, a flexible stent provided more feasible results. It was shown that the use of a flexible stent had a beneficial impact on the physical opening of the valve. Consequently, the GOA directly influenced the EOA of the valve, which in turn positively impacted the flow dynamics. The maximum stress during the complete systole phase was found in close proximity to the commissures and the curvature of the leaflet attachment onto the stent. These stress concentrations occur repeatedly due to the cyclic nature of the cardiac function, affecting the valve effectiveness and lifespan. Additionally, it was discovered that increasing the post height of the stent effectively reduced the maximum stress on the free edges of the leaflets. However, this adjustment resulted in a reduction in the GOA of the valve.

Deformation of leaflets with varying thickness exhibited enhanced pressure drop and decrease in stress concentration at the attachment point of the leaflet onto the stent towards the base of the valve, regurgitation, and velocity profiles. However, this design also displayed significant stress concentration at the thinner region near the valve's belly. Therefore, it is concluded that an optimized leaflet with predefined varying thickness to minimize areas with significant stress concentration would be the preferred option. An optimized radial curve of the leaflets could play a significant role in improving the valve performance. Ongoing research is focused on studying the behaviour of fluids, stents, and optimized leaflets as well as their interactions, with a fluid–structure interaction model being developed. Optimised designs will be manufactured through compression moulding.

Author Contributions: Conceptualization, L.R.M., W.d.P. and J.C.; methodology, L.R.M., W.d.P. and J.C.; software, L.R.M.; validation, L.R.M., W.d.P. and J.C.; formal analysis, L.R.M., W.d.P. and J.C.; writing—original draft preparation, L.R.M., W.d.P. and J.C.; writing—review and editing, L.R.M., W.d.P. and J.C.; supervision, W.d.P. and J.C. All authors have read and agreed to the published version of the manuscript.

Funding: This research was funded by South African Department of Science and Innovation through the Collaborative Program in Additive Manufacturing, grant number CSIR-NLC-CPAM-21-MOA-CUT-01.

Data Availability Statement: Further data that support the findings of this study are available from the corresponding author upon request.

Conflicts of Interest: The authors declare no conflicts of interest.

List of Acronyms, Abbreviations, and Units

CAD	Computer-aided design	
CFD	Computational fluid dynamics	
EOA	Effective orifice area	cm^2
FDA	Food and Drug Administration	
FEA	Finite element analysis	
GOA	Geometric orifice area	mm^2
ISO	International Organization for Standardization	
PCU	Polycarbonate urethane	

References

1. Schoen, F.J.; Fernandez, J.; Gonzalez-Lavin, L.; Cernaianu, A. Causes of Failure and Pathologic Findings in Surgically Removed Ionescu-Shiley Standard Bovine Pericardial Heart Valve Bioprostheses: Emphasis on Progressive Structural Deterioration. *Circulation* **1987**, *76*, 618–627. [CrossRef]
2. Bernacca, G.M.; Mackay, T.G.; Wilkinson, R.; Wheatley, D.J. Calcification and fatigue failure in a polyurethane heart valve. *Biomaterials* **1995**, *16*, 279–285. [CrossRef] [PubMed]
3. Piatti, F.; Sturla, F.; Marom, G.; Sheriff, J.; Claiborne, T.E.; Slepian, M.J.; Redaelli, A.; Bluestein, D. Hemodynamic and thrombogenic analysis of a trileaflet polymeric valve using a fluid-structure interaction approach. *J. Biomech.* **2015**, *48*, 3641–3649. [CrossRef] [PubMed]
4. Zebhi, B.; Lazkani, M.; Bark, D. Calcific Aortic Stenosis—A Review on Acquired Mechanisms of the Disease and Treatments. *Front. Cardiovasc. Med.* **2021**, *8*, 734175. [CrossRef] [PubMed]
5. Garcia, D.; Kadem, L. What Do You Mean by Aortic Valve Area: Geometric Orifice Area, Effective Orifice Area, or Gorlin Area? *J. Heart Valve Dis.* **2006**, *15*, 601.
6. Saikrishnan, N.; Kumar, G.; Sawaya, F.J.; Lerakis, S.; Yoganathan, A.P. Accurate assessment of aortic stenosis: A review of diagnostic modalities and hemodynamics. *Circulation* **2014**, *129*, 244–253. [CrossRef] [PubMed]
7. Wang, W.; Wang, C. *The Design and Manufacture of Medical Devices*; Elsevier: Amsterdam, The Netherlands, 2012. [CrossRef]
8. Mvondo, C.M.; Pugliese, M.; Giamberti, A.; Chelo, D.; Kuate, L.M.; Boombhi, J.; Dailor, E.M. Surgery for rheumatic mitral valve disease in sub-saharan African countries: Why valve repair is still the best surgical option. *Pan Afr. Med. J.* **2016**, *24*, 307. [CrossRef]
9. Kütting, M.; Roggenkamp, J.; Urban, U.; Schmitz-Rode, T.; Steinseifer, U. Polyurethane heart valves: Past, present and future. *Expert Rev. Med. Devices* **2011**, *8*, 227–233. [CrossRef]
10. Baura, G.D. Heart Valves. In *Medical Device Technologies*; Elsevier: Amsterdam, The Netherlands, 2012; pp. 121–145. [CrossRef]
11. Ghanbari, H.; Viatge, H.; Kidane, A.G.; Burriesci, G.; Tavakoli, M.; Seifalian, A.M. Polymeric heart valves: New materials, emerging hopes. *Trends Biotechnol.* **2009**, *27*, 359–367. [CrossRef]
12. Cardiovascular Implants-Cardiac Valve Prostheses-Part 3: Heart Valve Substitutes Implanted by Transcatheter Techniques Copyright Protected Document. 2021. Available online: www.iso.org (accessed on 31 May 2024).
13. Thubrikar, M.J.; Aouad, J.; Nolan, S.P. Comparison of the in vivo and in vitro mechanical properties of aortic valve leaflets. *J. Thorac. Cardiovasc. Surg.* **1986**, *92*, 29–36. [CrossRef]
14. ViVitroLabs.com, Pulse Duplicator Most Cited In-Vitro Cardiovascular Hydrodynamic Testing System. Available online: https://vivitrolabs.com/wp-content/uploads/2016/02/Pulse-Duplicator-Brochure-2016-VIVI-MKT-046.pdf (accessed on 7 July 2023).
15. Stasiak, J.R.; Serrani, M.; Biral, E.; Taylor, J.V.; Zaman, A.G.; Jones, S.; Ness, T.; De Gaetano, F.; Costantino, M.L.; Bruno, V.D.; et al. Design, development, testing at ISO standards and: In vivo feasibility study of a novel polymeric heart valve prosthesis. *Biomater. Sci.* **2020**, *8*, 4467–4480. [CrossRef]
16. Masheane, L.; Preez, W.D.; Combrinck, J. Assessment of manufacturability and performance of polyurethane heart valves produced through a locally developed dip moulding process. In Proceedings of the 17th RAPDASA Annual International Conference, Vanderbijlpark, South Africa, 2–4 November 2016.
17. Chandran, K.B. Role of Computational Simulations in Heart Valve Dynamics and Design of Valvular Prostheses. *Cardiovasc. Eng. Technol.* **2010**, *1*, 18–38. [CrossRef]

18. Salamatova, V.Y.; Liogky, A.A.; Karavaikin, P.A.; Danilov, A.A.; Kopylov, P.Y.; Kopytov, G.V.; Kosukhin, O.N.; Pryamonosov, R.A.; Shipilov, A.A.; Yurova, A.S.; et al. Numerical assessment of coaptation for auto-pericardium based aortic valve cusps. *Russ. J. Numer. Anal. Math. Model.* **2019**, *34*, 277–287. [CrossRef]
19. Chandran, K.B.; Kim, S.-H.; Han, G. Stress distribution on the cusps of a polyurethane trileaflet heart valve prosthesis in the closed position. *J. Biomech.* **1991**, *24*, 385–395. [CrossRef] [PubMed]
20. Rajiah, P.; Moore, A.; Saboo, S.; Goerne, H.; Ranganath, P.; MacNamara, J.; Joshi, P.; Abbara, S. Multimodality imaging of complications of cardiac valve surgeries. *Radiographics* **2019**, *39*, 932–956. [CrossRef] [PubMed]
21. Amabili, M.; Breslavsky, I.D.; Reddy, J.N. Nonlinear higher-order shell theory for incompressible biological hyperelastic materials. *Comput. Methods Appl. Mech. Eng.* **2019**, *346*, 841–861. [CrossRef]
22. Susin, F.M. Complete Unsteady One-Dimensional Model of the Net Aortic Pressure Drop. *Open Biomed. Eng. J.* **2019**, *13*, 83–93. [CrossRef]
23. Adda, J.; Stanova, V.; Habib, G.; Rieu, R. In vitro correlation between the effective and geometric orifice area in aortic stenosis. *J. Cardiol.* **2021**, *77*, 334–340. [CrossRef]
24. Gulbulak, U.; Gecgel, O.; Ertas, A. A deep learning application to approximate the geometric orifice and coaptation areas of the polymeric heart valves under time–varying transvalvular pressure. *J. Mech. Behav. Biomed. Mater.* **2021**, *117*, 104371. [CrossRef]
25. Masheane, L.; Preez, W.D.; Combrinck, J. Implementation of a digital twinning approach to improve designs of polyurethane heart valves. *S. Afr. J. Ind. Eng.* **2023**, *34*, 104–115. [CrossRef]
26. Nader, E.; Skinner, S.; Romana, M.; Fort, R.; Lemonne, N.; Guillot, N.; Gauthier, A.; Antoine-Jonville, S.; Renoux, C.; Hardy-Dessources, M.-D.; et al. Blood rheology: Key parameters, impact on blood flow, role in sickle cell disease and effects of exercise. *Front. Physiol.* **2019**, *10*, 1329. [CrossRef]
27. Butera, G.; Chessa, M.; Eicken, A.; Thomson, J.D. *Atlas of Cardiac Catheterization for Congenital Heart Disease*; Springer International Publishing: Cham, Switzerland, 2019.
28. Berg, M.; Holroyd, N.; Walsh, C.; West, H.; Walker-Samuel, S.; Shipley, R. Challenges and opportunities of integrating imaging and mathematical modelling to interrogate biological processes. *Int. J. Biochem. Cell Biol.* **2022**, *146*, 106195. [CrossRef] [PubMed]
29. Faure, M.E.; Suchá, D.; Schwartz, F.R.; Symersky, P.; Bogers, A.J.J.C.; Gaca, J.G.; Koweek, L.M.; de Heer, L.M.; Budde, R.P.J. Surgically implanted aortic valve bioprostheses deform after implantation: Insights from computed tomography. *Eur. Radiol.* **2020**, *30*, 2651–2657. [CrossRef] [PubMed]
30. Schoen, F.J.; Levy, R.J. Calcification of tissue heart valve substitutes: Progress toward understanding and prevention. *Ann. Thorac. Surg.* **2005**, *79*, 1072–1080. [CrossRef] [PubMed]
31. Jafar, R.; Labrosse, M.R.; Weaver, J.D.; Retta, S.M.; Wu, C.; Duraiswamy, N. A computational study on deformed bioprosthetic valve geometries: Clinically relevant valve performance metrics. *J. Biomech. Eng.* **2020**, *142*, 011003. [CrossRef] [PubMed]
32. Tao, L.; Jingyuan, Z.; Hongjun, Z.; Yijing, L.; Yan, X.; Yu, C. Research on fatigue optimization simulation of polymeric heart valve based on the iterative sub-regional thickened method. *Int. J. Numer. Method Biomed. Eng.* **2023**, *39*, e3717. [CrossRef]
33. Yousefi, A.; Bark, D.L.; Dasi, L.P. Effect of Arched Leaflets and Stent Profile on the Hemodynamics of Tri-Leaflet Flexible Polymeric Heart Valves. *Ann. Biomed. Eng.* **2017**, *45*, 464–475. [CrossRef]

Disclaimer/Publisher's Note: The statements, opinions and data contained in all publications are solely those of the individual author(s) and contributor(s) and not of MDPI and/or the editor(s). MDPI and/or the editor(s) disclaim responsibility for any injury to people or property resulting from any ideas, methods, instructions or products referred to in the content.